Bridgelike Interconnections between Thick Filaments in Stretched Skeletal Muscle Fibers Observed by the Freeze-Fracture Method

Suechika Suzuki and Gerald H. Pollack

Center for Bioengineering, University of Washington, Seattle, Washington 98195. Dr. Suzuki's present address is Department of Physiology, School of Medicine, Teikyo University, Itabashi-ku, Tokyo 173, Japan.

Abstract. The ultrastructure of frog semitendinosus muscle was explored using the freeze-fracture, deep-etch, rotary-shadowing technique. Mechanically skinned fibers were stretched to decrease or eliminate the overlap of thick and thin filaments before rapid freezing with liquid propane. In relaxed, contracting, and rigor fibers, a significant number of bridgelike interconnections, distinct from those observed in the M-region, were observed between adjacent thick filaments in the non-overlap region. Their half-length and diameter corresponded approximately to the known dimensions of the cross-bridge (or myosin S-1). The interconnection may thus be formed by the binding of two apposed cross-bridges projecting from adjacent thick filaments. Fixation with 0.5% glutaraldehyde for 5–10 min before freezing effectively preserved these structures. The results indicate that the interconnections are genuine structures that appear commonly in stretched muscle fibers. They may play a role in stabilizing the thick filament lattice, and possibly in the contractile process.

An electron microscopic study of muscle published some time ago (11) drew attention to the presence of rung-like interconnections between adjacent thick filaments. These resembled the M-bridges, which interconnect thick filaments at their mid-length, but were located in flanking regions of the A-band. Comparable structures have appeared in other published micrographs (23), but little attention has been paid to them.

New interest has been sparked by a recent report that isolated myosin heads can form end-to-end dimers (21). This observation raises the intriguing possibility that the interconnections may be created by the binding of apposed cross-bridges at their tips.

To observe these structures with improved reliability and clarity, we used the freeze-fracture, deep-etch, rotary-shadowing method (8, 10, 17). This approach circumvents potential artifacts attendant upon conventional procedures and allows the interconnections to be studied with high resolution.

Materials and Methods

Single fibers were isolated from the semitendinosus muscle of the frog *Rana temporaria* in Ringer's solution. They were then transferred into a relaxing solution of the following composition (millimolar): KCl, 110; $MgCl_2$, 3; EGTA, 5; ATP, 2.5; imidazole, 10 (pH 7.0). Next, the fibers were mechanically skinned and mounted horizontally in a small experimental chamber (~0.05 ml) submersed in a bath of relaxing solution. One end of the fiber was connected to a fixed support and the other to a hook, movable by the regulation of a coiled spring. Both were integral parts of the experimental chamber.

Initially, the fiber was stretched with the movable hook. Then its central section was carefully sandwiched between two gold plates (Balzers, Hudson, NH), one of which contained a trough, milled to accommodate the fiber. The plates provided mechanical protection during jet freezing and support for the specimen in the fracture machine. Some fibers were left in relaxing solution; others were exposed to a contracting solution (pCa 5.7), prepared by the addition of $CaCl_2$ to the relaxing solution. Still others were studied in the unskinned condition, activated with 80 mM K^+. (At low temperature, this results in a sustained contracture). The above-mentioned preparations were either lightly fixed with 0.5% glutaraldehyde for 10 min before freezing or left unfixed.

The experimental chamber (with gold plate sandwich) was removed from the bath, quickly blotted and transferred to a dual jet liquid propane freezing device (designed by Müller et al. [22] and modified by J. Gilkey and A. Staehelin), and frozen rapidly by jetting liquid propane at about −190°C.

The experimental chamber was plunged into liquid nitrogen, where the gold plate sandwich was removed and split apart. Samples were stored under liquid nitrogen. Fracturing took place in a freeze-fracture unit (BAF 301, Balzers, Liechtenstein) at $<10^{-6}$ torr. After etching for 3–4 min at −95°C, the specimen was rotary shadowed with Pt/C at an angle of 20–40° from the horizontal. Then pure carbon was deposited at 90°. The thickness of the Pt/C layer was estimated from micrographs using images of fused filaments (9). The shadowed muscle tissue was dissolved by immersion into Clorox household bleach (5.25% sodium hypochlorite) diluted to 50%.

Replicas were observed using a JEOL 100C electron microscope at 100 kV. Negatives were routinely contact-reversed and then printed to give negative images. Quantitative measurements were made from one representative field per condition.

To confirm earlier reports, some resin-embedded, ultrathin sections, which were prepared from stretched fibers fixed with 2.5% glutaraldehyde and post-fixed with 2% OsO_4, were also examined.

Results

Fig. 1 *a* shows a section of a chemically fixed, relaxed fiber in which the sarcomeres had been stretched to withdraw the thin

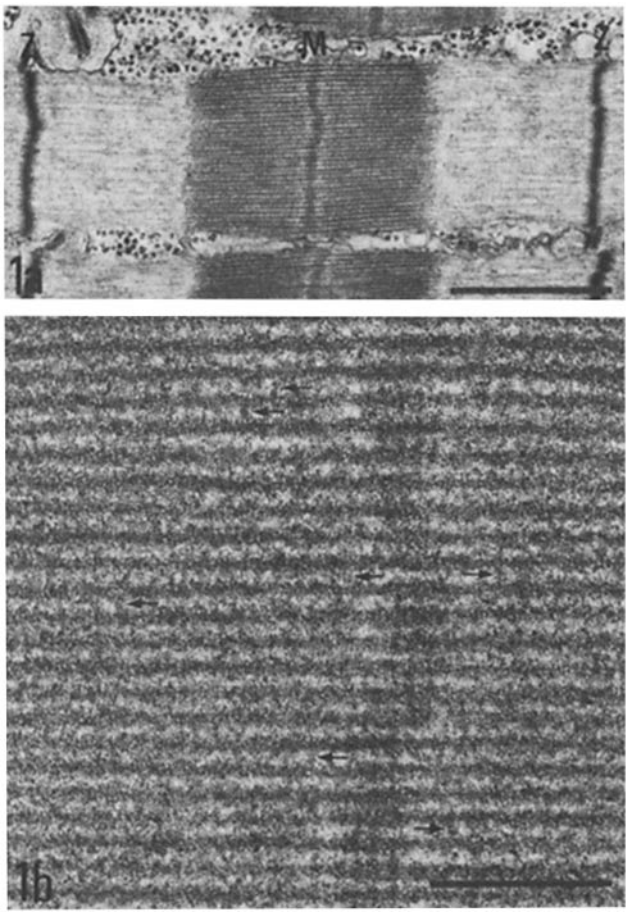

Figure 1. Longitudinal section of a stretched, intact, frog semitendinosus fiber fixed with glutaraldehyde and OsO_4 in the relaxed state. (*a*) Low magnification view, sarcomere length, 3.52 μm. Note that there is no overlap of thick and thin filaments. *M*, M-region. *Z*, Z-band. Bar, 1 μm. (*b*) High magnification view of the A-band shown in *a*. Apparent interconnections between thick filaments are observed (see arrows for some examples). Bar, 0.2 μm.

filaments from the A-band. In some parts of the A-band, electron-dense bridgelike structures, similar in appearance to the bridges found in the M-region, are observed between adjacent thick filaments (Fig. 1 *b*). However, the possibility of superposed structures and the presence of noise generated by soluble proteins limited our ability to define these structures more precisely.

Fig. 2 *a* shows a freeze-fracture replica image of sarcomere comparable to that shown in Fig. 1. Thick, thin, and connecting filaments are well resolved. Filament lengths were 1.58 μm (thick), and 0.95 μm (thin), in good agreement with established values.

Fig. 2 *b* reveals additional detail. Many cross-bridges are arrayed helically along the thick filament. The helix is right handed (arrows), and the gyres are inclined at ~30° to the filament axis, in agreement with published values (7, 16, 28). In addition, interconnections between thick filaments can be seen scattered throughout the field. The most proximal ones occur some 80 nm from the center of the M-region, whereas the most distal ones occur at the ends of the thick filaments (see also Fig. 4).

The characteristics of the interconnections are clearly revealed at high magnification in Fig. 2 *c*. They are rodlike and run from one thick filament to an adjacent one. Stereo images (±10°) confirmed that the interconnections could not have arisen out of two shorter, superposed structures. After correction for the Pt layer (2.8 nm in this field), the dimensions of the interconnections were ~6.5 nm in diameter and ~27.5 nm in length. Occasionally, a fine stripe of low electron density, which appears as a dark line on this negative image, was observed midway along the interconnection, implying the fusion of two, shorter structures projecting from adjacent thick filaments.

Measured structural parameters, including dimensions, angles, and numbers of interconnections are schematized in Fig. 3 and summarized in Table I. The Table also includes data obtained in the other physiological states described below. Since not all regions of each micrograph were clear, measurements were restricted to regions in which thick filaments were well defined and clearly separated.

Fig. 4 shows a replica from a relaxed fiber that was chemically fixed before freezing. The result is similar to the unfixed case, except that the number of interconnections per unit length is somewhat higher (Table I).

Replicas of contracting fibers are shown in Figs. 5 and 6. In the first, contraction was induced by the exchange of relaxing solution for contracting solution. In the second, the single, unskinned fiber was activated by K^+ at 5°C for 10 s and then lightly fixed in 0.5% glutaraldehyde contained within the high-K solution for 10 min before freezing. In both cases many interconnections were observed (Figs. 5 and 6).

As shown in Table I, the dimensions of the interconnections in the contracting fibers were similar to those obtained in the relaxed fibers. The distribution of interconnection angles was also in the same range. There was no significant difference between the number of interconnections in the chemically fixed and unfixed contracting specimens; both were the same as the number in chemically fixed, relaxed fibers.

Several additional states were investigated (see Table I). Fibers frozen in rigor showed interconnections of the same character, dimension, and frequency as in the contracting state. Fibers were also frozen in solutions of low and zero ionic strength to increase the spacing between thick filaments. Again, comparable results were found, except for the longer span between thick filaments and commensurately longer interconnections. In distilled water, despite a remarkable swelling, interconnections were still observed, though fewer in number. Because interconnections could be observed in such salt-free media, the trabeculum-like artifact identified by Miller et al. (19) can be ruled out.

Discussion

Although interconnections between thick filaments have been apparent on electron micrographs for some time (4, 11, 15, 17, 25; see also Fig. 8 of reference 23), no systematic attempt to confirm these structures has yet been made. The present work has revealed that interconnections between thick filaments are genuine structures that appear under a variety of physiological conditions—in partially and fully stretched fibers, during relaxation, contraction and rigor.

The interconnections were generally rodlike; they were typically four to five times as long as they were wide, though longer interconnections were observed when the interfilament span was larger. Their orientation was primarily normal to

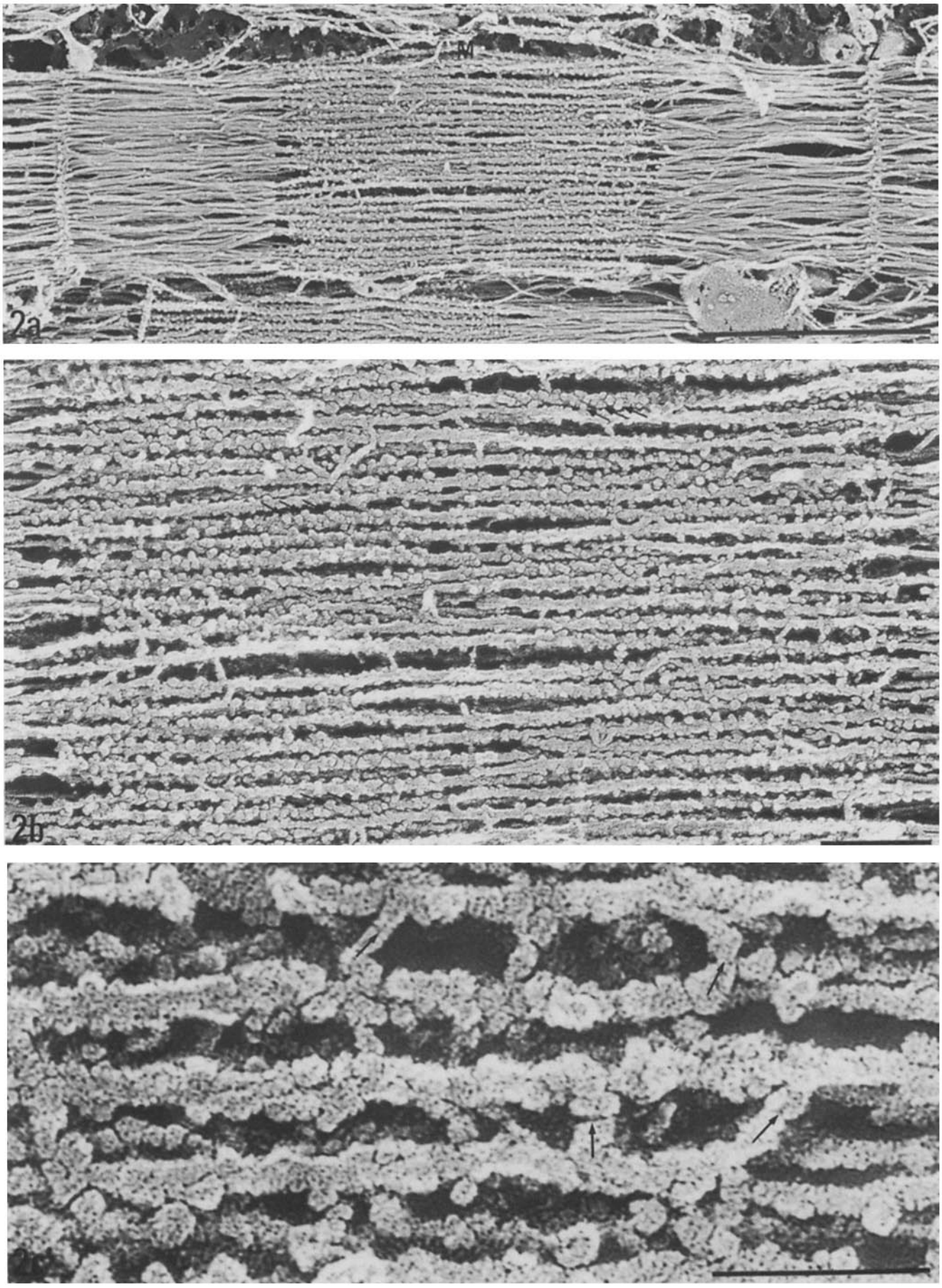

Figure 2. Freeze-fracture replica of a stretched sarcomere in a mechanically skinned, relaxed fiber frozen without chemical fixation, showing interconnections between thick filaments. (*a*) Low magnification view of the sarcomere, showing no overlap of thick and thin filaments. Sarcomere length, 3.52 μm. *M*, M region. *Z*, Z-band. Bar, 1 μm. (*b*) High magnification view of the A-band. Interconnections are observed between thick filaments, outside of the M-region. Note also the cross-bridges located on the thick filaments. Arrows indicate the right handed cross-bridge helix. Bar, 0.2 μm. (*c*) Enlarged view of a portion of the A-band, showing some interconnections with apparent binding faces (arrows) midway along their length. Bar, 0.1 μm.

the fiber axis, with substantial, apparently random, variation around this mean (Table I). Differences in physiological states had no notable effect on any aspect of the interconnection, except, perhaps, that their incidence was relatively lower in the relaxed, unfixed state (but see below). Links between filaments could also be observed in the overlap region, but it was difficult to define whether or not they interconnected thick filaments.

The origin of the interconnection is not yet certain. One possibility is that it is formed by an S-2 "peeling" off a thick filament, thereby allowing the tip of the S-1 head to reach the adjacent thick filament. If so, the interconnection should have been considerably broader at one end than at the other. In general, however, the interconnections were relatively uniform along their length.

Another possibility is that the interconnection is formed by the binding of two S-1's, protruding from adjacent thick filaments. Measured dimensions were typically 5.0–6.5 nm in diameter and 12–16 nm in half-length. These values are slightly higher than those for S-1 measured from isolated

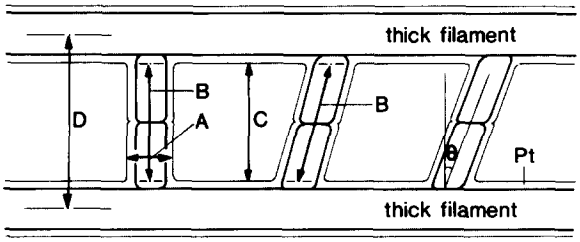

Figure 3. Diagrammatic representation of observed structures, illustrating the measured parameters. *A*, diameter of interconnections including Pt thickness. *B*, length of interconnections before correction for Pt thickness. *C*, interfilament space before subtraction of Pt thickness. *D*, center-to-center distance between thick filaments. θ, angle of interconnections, measured as deviation from the plane normal to the filament axis. *Pt*, platinum layer.

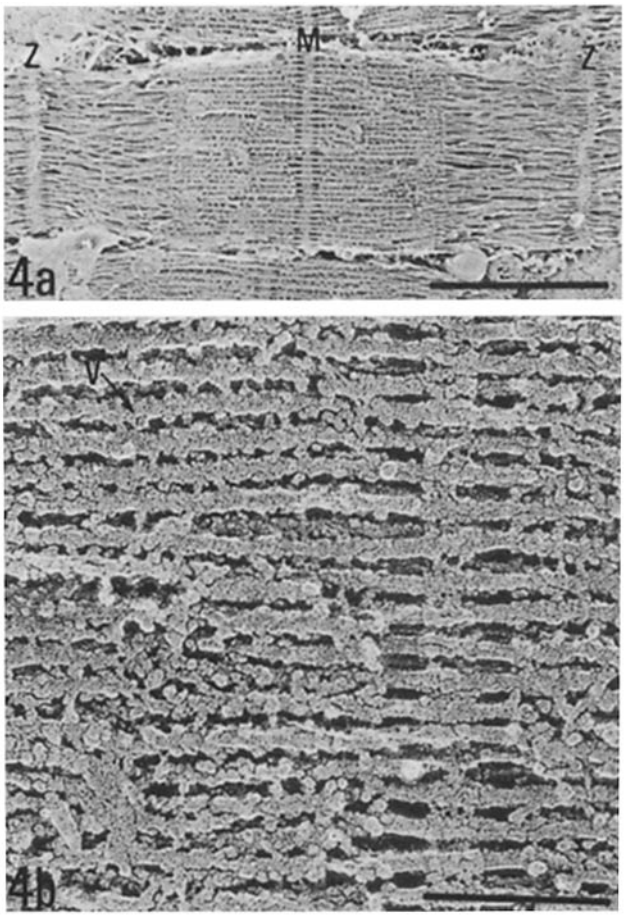

Figure 4. Stretched sarcomere of a relaxed fiber fixed lightly with glutaraldehyde. (*a*) Low magnification view; sarcomere length, 3.13 μm. Note the modest overlap of thick and thin filaments. *M*, M-region. *Z*, Z-band. Bar, 1 μm. (*b*) High magnification view of the A-band, showing the interconnections in the non-overlap region. Bar, 0.2 μm. Note occasional V-shaped interconnections (*V*).

Table I. Structural Parameters

			Interconnection					
Physiological condition	Fixation	Sarcomere length	*n*	Diameter	Length	Angle	Interval along thick filament	Level of significance against standard
		μm		*nm*	*nm*	*degrees*	*nm*	
Relaxed	−	3.52	131	12.16 ± 2.88 [6.5]	21.95 ± 7.35 [27.5]	22.3 ± 14.0	87.7 ± 22.6	<0.001
Relaxed	+	3.84	100	10.06 ± 2.81 [5.7]	23.70 ± 6.29 [28.1]	8.9 ± 8.7	38.1 ± 15.3	Standard
Contracting	−	4.03	100	11.49 ± 2.03 [5.9]	27.23 ± 7.29 [32.8]	13.6 ± 11.3	37.7 ± 17.9	>0.8
Contracting	+	3.57	100	9.18 ± 1.31 [5.0]	22.02 ± 4.79 [26.2]	12.5 ± 11.9	36.1 ± 18.7	>0.05
Rigor	+	3.16	60	9.74 ± 1.98 [5.1]	20.13 ± 4.29 [24.4]	9.6 ± 8.5	34.4 ± 17.9	>0.001
Low ionic strength	+	3.33	60	10.64 ± 2.08 [5.8]	27.33 ± 6.62 [32.1]	11.7 ± 11.9	38.4 ± 16.5	>0.9
Distilled water	−	2.94	60	7.86 ± 1.96 [3.9]	47.59 ± 17.68 [51.6]	17.0 ± 11.7	86.0 ± 28.7	<0.001
Thin section*	++	3.52	50	—	—	—	30.5 ± 10.0	<0.001

Values are mean ± SD. See Fig. 3. Values in brackets are dimensions after correction for Pt thickness. + indicates that the fiber was lightly fixed with glutaraldehyde; − indicates no fixation; ++ indicates double fixation with glutaraldehyde and OsO_4. Angles were measured as absolute value of deviation from the plane normal to the filament axis. *n*, number of interconnections studied.

* This result may represent an overestimate, as superposition effects may give rise to apparent interconnections.

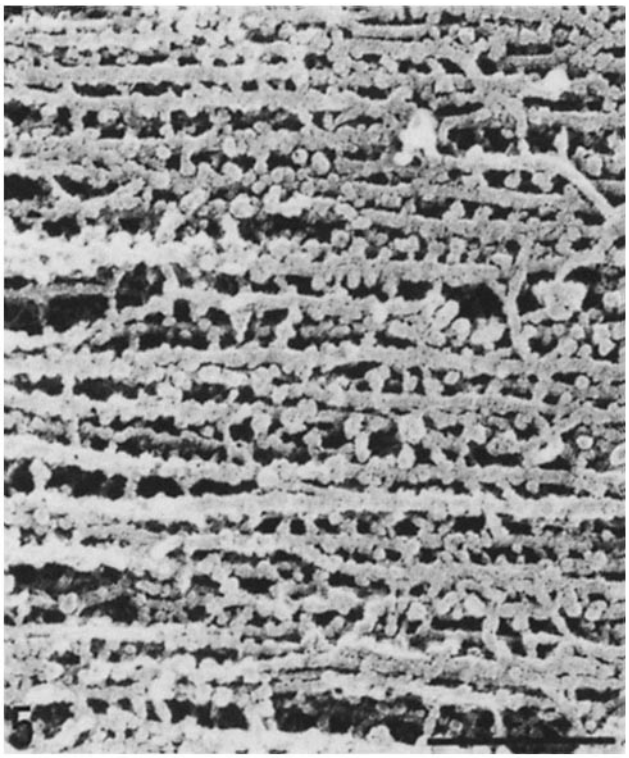

Figure 5. A portion of the non-overlap A-band of a fiber frozen in the activated state (pCa 5.7) without chemical fixation. Note the presence of interconnections. Sarcomere length, 4.03 μm. Bar, 0.2 μm.

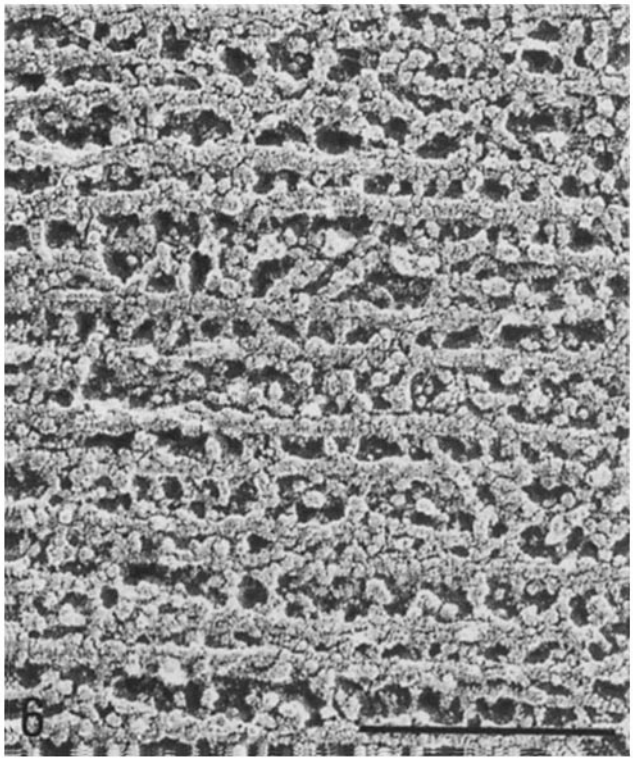

Figure 6. High magnification view of non-overlap A-band in an intact fiber lightly fixed with glutaraldehyde during contraction induced by high K and then frozen. Sarcomere length, 3.57 μm. Abundant interconnections are evident. Bar, 0.2 μm.

myosin molecules (5), but similar to the 5.5 and 12 nm obtained from image reconstruction of S-1 binding to thin filaments (20, 29), a situation closer perhaps to the one in situ. This dimensional consistency gives credibility to the possibility that the interconnection is formed by the binding of two single S-1's at their tips. The stripe of low electron density sometimes observed midway along the interconnection may represent the binding face of the two bridges. Biochemical evidence supports this possibility. There are reports of head-to-head interaction in myosin filaments (26), and aggregation or dimerization of isolated myosin S-1 (1, 6, 18, 21). According to Morel and Garrigos (21), the dimer of myosin S-1 predominates in the monomer-dimer mixture under physiological conditions.

An altogether different possibility is that the interconnection is a nonmyosin "strut" (17), consisting of C-protein. The distribution of C-protein, however, is restricted to a zone in each half sarcomere that begins some 180 nm (2, 27) or occasionally slightly less (3) from the M-region and ends ~250 nm from the filament tip. In contrast, the interconnections observed here extended over the entire length of the filament except for the small central bare zone. Thus, at least some of the interconnections cannot be C-protein struts.

On the other hand, the zone of distribution of interconnections is coincident with the zone of distribution of myosin heads. Furthermore, the interconnections are so dominant in at least some of the micrographs (e.g., Figs. 5 and 6) that it is difficult to envision them as anything other than the most abundant protein in the thick filament, namely myosin. Nevertheless, this assignment must necessarily remain tentative until the chemical composition has been definitively ascertained.

Another noteworthy feature was the interconnection distribution (Table I). In most instances the repeat interval was close to 43 nm, the value expected from x-ray diffraction (14). The lower incidence in some cases, including long bare stretches in some relaxed fibers (e.g., Fig. 2), could be genuine; on the other hand, artifactual sources must be considered. The strong physical forces associated with ice crystal growth and with fracture may tend to disrupt interconnections. This is supported by the frequently observed destruction of M-bridges (Fig. 2), by the appearance of "bumpy" regions along thick filaments, where broken interconnections appear to have retracted, and by the absence of reduced incidence in relaxed fibers whose structure had been stabilized with glutaraldehyde before freezing (Table I).

Several potentially more serious artifacts were also considered. Apparent interconnections could be formed by Pt bridges between structures projecting from adjacent thick filaments but not touching. Since the shadow was 2.0–2.8 nm thick, structures separated by up to 5.6 nm could be so joined. Two observations argue against this. First, unless the complementary projections pointed precisely toward one another, the artificially bridged interconnection should have shown kinks or offsets at their midpoints. Only occasionally were such midpoint kinks apparent (e.g. Fig. 2*c*). Second, interconnections could be found between filaments that were widely separated, either fortuitously or otherwise (low or zero ionic strength). In such instances, the Pt bridge would have had to be an order of magnitude longer than when the interfilament separation was normal.

The possibility that the interconnections are artifacts induced by chemical fixation has been considered by Magid et al. (17). Since the interconnections could be observed in fibers frozen in the absence of any chemical fixation, this possibility is excluded.

The role of the interconnections is, at this stage, unclear. Certainly these structures will serve to stabilize the thick filament lattice, as suggested earlier (17). If the interconnections persist in the overlap zone during contraction, then actomyosin interaction may need to be explained by mechanisms different from the ones currently envisioned (12–14), for cross-bridge rotation would be implausible. How contractile force might be generated would then be a matter for speculation (24).

We thank Drs. J. K. Koehler (University of Washington), P. Cullus, M. Hope, and B.H. Bressler (University of British Columbia) for providing the Balzers Freeze-Etch facilities, and Dr. D. E. Johnson (University of Washington) for the use of the JEOL electron microscope. We thank also Dr. M. E. Cantino (University of Washington) for her helpful suggestions in implementing the freeze-fracture method, Mr. P. H. Baatsen for his technical assistance, and Mr. S. K. Richmond for his darkroom work.

This work was supported in part by grants from the National Institutes of Health (HL 18676), the American Heart Association (82726), and the Yamada Science Foundation, Osaka.

Received for publication 19 April 1985, and in revised form 5 November 1985

References

1. Barrett, T. W., W. L. Peticolas, and J. Robson. 1978. Laser Raman light-scattering observations of conformational changes in myosin induced by inorganic salts. *Biophys. J.* 23:349–358.

2. Craig, R. 1977. Structure of A-segments from frog and rabbit skeletal muscle. *J. Mol. Biol.* 109:69–81.

3. Dennis, J. E., T. Shimizu, F. C. Reinach, and D. A. Fischman. 1984. Localization of C-protein isoforms in chicken skeletal muscle: ultrastructural detection using monoclonal antibodies. *J. Cell Biol.* 98:1514–1522.

4. Egginton, S., and I. A. Johnston. 1982. A morphometric analysis of regional differences in myotomal muscle ultrastructure in the juvenile eel (*Anguilla anguilla L.*). *Cell Tissue Res.* 222:579–596.

5. Elliott, A., and G. Offer. 1978. The shape and flexibility of the myosin molecule. *J. Mol. Biol.* 123:505–519.

6. Flamig, D. P., and M. A. Cusanovich. 1981. Aggregation-linked kinetic heterogeneity in bovine cardiac myosin subfragment 1. *Biochemistry.* 20:6760–6767.

7. Haselgrove, J. C. A. 1980. A model of myosin cross-bridge structure consistent with the low-angle X-ray diffraction pattern from vertebrate muscle. *J. Muscle Res. Cell Motil.* 2:177–191.

8. Heuser, J. E. 1983. Structure of the myosin crossbridge lattice in insect flight muscle. *J. Mol. Biol.* 169:123–154.

9. Heuser, J. E. 1983. Procedure for freeze-drying molecules adsorbed to mica flakes. *J. Mol. Biol.* 169:155–195.

10. Heuser, J. E., and P. Cooke. 1983. Actin-myosin interactions visualized by the quick-freeze, deep-etch replica technique. *J. Mol. Biol.* 169:97–122.

11. Hoyle, G., P. A. McNeill, and A. I. Selverston. 1973. Ultrastructure of barnacle giant muscle fibers. *J. Cell Biol.* 56:74–91.

12. Huxley, A. F., and R. M. Simmons. 1971. Proposed mechanism of force generation in striated muscle. *Nature (Lond.).* 233:533–538.

13. Huxley, H. E. 1969. The mechanism of muscular contraction. *Science (Wash. DC).* 164:1356–1366.

14. Huxley, H. E., and W. Brown. 1967. The low angle X-ray diagram of vertebrate striated muscle and its behavior during contraction and rigor. *J. Mol. Biol.* 30:383–434.

15. Ishikawa, H. 1980. Fine structure of the stretched myofibril as revealed by high voltage electron microscopy. *Biomed. Res.* 1:15–23.

16. Kensler, R. W., and M. Stewart. 1983. Frog skeletal muscle thick filaments are three-stranded. *J. Cell Biol.* 96:1797–1802.

17. Magid, A., H. P. Ting-Beall, M. Carvell, T. Kontis, and C. Lucaveche. 1984. Contracting filaments, core filaments, and side-struts: a proposal to add three new load-bearing structures to the sliding filament model. *In* Contractile Mechanism in Muscle. G. H. Pollack and H. Sugi, editors. Plenum Publishing Corp., New York. 307–328.

18. Margossian, S. S., and S. Lowey. 1977. Calcium-induced aggregation of myosin subfragments. *Biophys. J.* 17(2, Pt. 2:)37a. (Abstr.)

19. Miller, K. R., C. S. Prescott, T. L. Jacobs, and N. L. Lassignal. 1983. Artifacts associated with quick-freezing and freeze-drying. *J. Ultrastruct. Res.* 82:123–133.

20. Moore, P. B., H. E. Huxley, and D. J. DeRosier. 1970. Three dimensional reconstruction of F-actin, thin filaments and decorated thin filaments. *J. Mol. Biol.* 50:279–295.

21. Morel, J. E., and M. Garrigos. 1982. Dimerization of the myosin heads in solution. *Biochemistry.* 21:2679–2686.

22. Müller, J. E., N. Meister, and H. Moore. 1980. Freezing in a propane jet and its application in freeze-fracturing. *Mikroskopie.* 36:129–140.

23. Pollack, G. H. 1983. The cross-bridge theory. *Physiol. Rev.* 63:1049–1113.

24. Pollack, G. H. 1984. A proposed mechanism of contraction in which stepwise shortening is a basic feature. *In* Contractile Mechanisms in Muscle. G. H. Pollack, and H. Sugi, editors. Plenum Publishing Corp., New York. 787–792.

25. Salviati, G., M. M. Sorenson, and A. B. Eastwood. 1982. Calcium accumulation by the sarcoplasmic reticulum in two populations of chemically skinned human muscle fibers: effects of calcium and cyclic AMP. *J. Gen. Physiol.* 79:603–632.

26. Schaub, M. C., and T. G. Watterson. 1976. Evidence for head-head interaction in intact myosin. *In* Contractile Systems in Nonmuscle Tissues. S. V. Perry, A. Margreth, and R. S. Adelstein, editors. Elsevier/North-Holland Biomedical Press, Amsterdam. 343 (Abstr.)

27. Sjostrom, M., and J. M. Squire. 1977. Fine structure of the A-band in cryosections. The structure of the A-band of human skeletal muscle fibers from ultra-thin cryo-sections negatively stained. *J. Mol. Biol.* 109:49–68.

28. Squire, J. M. 1975. Muscle filament structure and muscle contraction. *Annu. Rev. Biophys. Bioeng.* 4:137–163.

29. Taylor, K. A., and L. A. Amos. 1981. A new model for the geometry of the binding of the myosin crossbridges to muscle thin filaments. *J. Mol. Biol.* 147:297–324.